Journal of Alloys and Compounds 501 (2010) 54–59

Contents lists available at ScienceDirect

Journal of Alloys and Compounds

journal homepage: www.elsevier.com/locate/jallcom

# Characteristics of doped $TiO_2$ photocatalysts for the degradation of methylene blue waste water under visible light

Zhongqing Liu[a,b,*], Yicao Wang[b], Wei Chu[a], Zhenhua Li[b], Changchun Ge[b]

[a] *School of Chemical Engineering, Sichuan University, Chengdu 610065, China*
[b] *School of Materials Science and Technology, University of Science and Technology Beijing, Beijing 100083, China*

ARTICLE INFO

*Article history:*
Received 6 January 2010
Received in revised form 29 March 2010
Accepted 2 April 2010
Available online 10 April 2010

*Keywords:*
N-doped $TiO_2$ catalyst
Photocatalytic degradation
Electron structure
Density functional simulation
Density of states (DOS)

ABSTRACT

Fe-doped, N-doped, (Fe,N)-codoped and undoped $TiO_2$ were prepared by a hydrothermal treatment, followed by a calcination process, using $TiOSO_4$, $CO(NH_2)_2$ and $Fe(NO_3)_3$ as raw materials. The samples were characterized by XRD, XPS, TEM, PL, FT-IR and UV-Vis diffuse reflectance spectra. Photocatalytic experiments were carried out by decomposition of methylene blue aqueous solution under visible light. It was found that as-prepared $TiO_2$-based catalysts were single phasic anatase titania. Among these samples, the N-doped $TiO_2$ exhibited the better photocatalytic activity. The relations of their photocatalytic activity, spectroscopy properties and band gap structures have been discussed while *ab initio* calculations of electron structure and density of state (DOS) were done by DFT quantum chemistry method.

## 1. Introduction

In recent years, $TiO_2$-based catalysts have attracted increasing attentions due to their prominent application prospects in the areas of degradation of pollutants in water and air, photoelectrochemical splitting of water and photoelectric conversion. Unfortunately, $TiO_2$ exhibits catalytic activity only under ultraviolet light because it has a band gap of 3.2 eV, failing to use visible light accounting for near 50% of sunlight spectrum. Therefore, a large amount of investigations aiming at narrowing band gap of $TiO_2$ to response to visible light have been carried out, using dopants. Up to now, several types of dopants, including transitional metal ions, alkali metal additives, nonmetal promoters as well as metal and nonmetal co-dopants (such as La/Sr and N) have been studied to prepare codoped $TiO_2$ photocatalysts. Among metal dopants, Fe (β) has been thought to be an excellent dopant [1–7] because doped $Fe^{3+}$ replaces $Ti^{4+}$ in $TiO_2$ lattice, forming localized bands near the bottom of conduction band and thereby decreasing band gap. For nonmetal dopants, N is found to be an outstanding candidate, in respect that doped N can not only broaden wavelength responded scope but also not debase photocatalytic activity under ultraviolet light [8–15]. However, $TiO_2$ photocatalysts codoped with metal ions such as $Fe^{3+}$ and nometal species such as N have been few researched [16–18]. In our previous work [17], although (metal, N)-codoped $TiO_2$ catalysts have been fabricated by sol-gel auto-ignition route, they are mixed phases with anatase and rutile due to a high preparation temperature close to 1000 °C in auto-ignition process. In present work, a different preparation method was used to prepare $TiO_2$-based photocatalysts with a single phasic anatase. The relations of photocatalytic activity, spectroscopy properties and band gap structures of the catalysts have been discussed while *ab initio* calculations of electron structures were carried out by DFT method.

## 2. Experimental

$TiOSO_4$, $CO(NH_2)_2$ and $Fe(NO_3)_3$ with chemical grade, were used in our experiments without further purification. In a typical process, solution of $TiOSO_4$ and $CO(NH_2)_2$ was moved into a 500 mL Teflon-lined stainless autoclave. The concentration of $TiOSO_4$ was 0.5 mol $L^{-1}$ and the molar ratio of $TiOSO_4$ to $CO(NH_2)_2$ was 1:5. After the autoclave was sealed, it was heated at 160 °C for 6 h. Subsequently, the product was taken out and washed with distilled water and absolute ethanol repeatedly to make $TiO_2 \cdot nH_2O$ free of sulphate ions. To fabricate undoped $TiO_2$ powders, the washed product was dried in an oven at 120 °C for 12 h and calcined at 500 °C for 2 h in a muffle furnace under an aerated condition. To prepare N-doped $TiO_2$ catalyst, the dried $TiO_2$ powders from hydrothermal process were mixed with $CO(NH_2)_2$ at a molar ratio of 1:1 before they were calcined at 500 °C for 2 h. Correspondingly, Fe-doped $TiO_2$ was prepared by adding $Fe(NO_3)_3$ to the solution of $TiOSO_4$ and $CO(NH_2)_2$ before hydrothermal treatment. (Fe,N)-codoped $TiO_2$ was synthesized using the same conditions and procedure as that of preparing N-doped $TiO_2$ except for that $Fe(NO_3)_3$ was added to the solution of $TiOSO_4$ and $CO(NH_2)_2$ prior to hydrothermal treatment. The quantity of $Fe(NO_3)_3$ was 1.0 at.% according to the formula: $M_{Fe}/(M_{Fe}+M_{Ti})$, where $M_{Fe}$ and $M_{Ti}$ were mole number of $Fe(NO_3)_3$ and $TiOSO_4$ used in our experiments, respectively.

---

* Corresponding author at: School of Chemical Engineering, Sichuan University, Chengdu 610065, China. Tel.: +86 21 8540 0422; fax: +86 21 8540 0422.
*E-mail address:* 301qzl@vip.sina.com (Z.Q. Liu).

0925-8388/$ – see front matter © 2010 Elsevier B.V. All rights reserved.
doi:10.1016/j.jallcom.2010.04.027

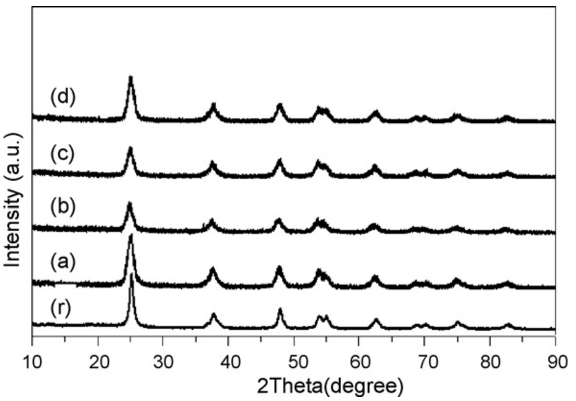

**Fig. 1.** XRD patterns of (r) anatase titania, (a) undoped $TiO_2$, (b) N-doped $TiO_2$, (c) Fe-doped $TiO_2$ and (d) (Fe,N)-codoped $TiO_2$.

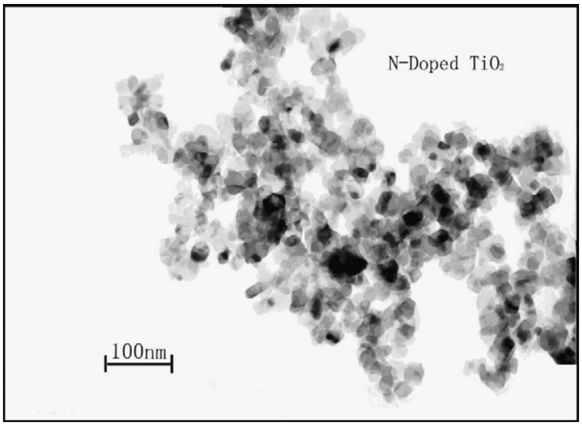

**Fig. 2.** TEM image of the N-doped $TiO_2$ powders.

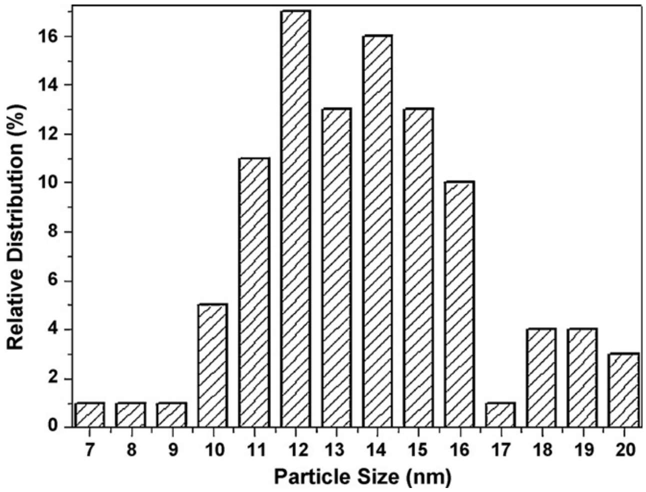

**Fig. 3.** Particle size distribution histogram of the N-doped $TiO_2$.

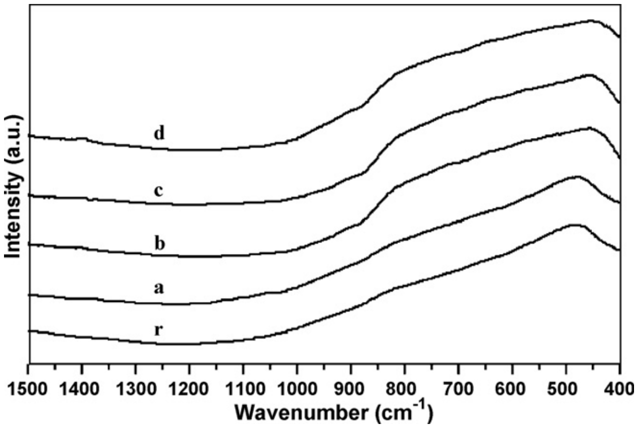

**Fig. 4.** FT-IR spectra of (r) anatase titania, (a) undoped $TiO_2$, (b) N-doped $TiO_2$, (c) Fe-doped $TiO_2$ and (d) (Fe,N)-codoped $TiO_2$.

The samples were characterized by several techniques: X-ray powder diffraction (XRD; Rigaku D/Max-RB, Japan) with $CuK_\alpha$ radiation ($\lambda = 0.15406$ nm), X-ray photoemission spectroscopy (XPS, VG ESCALAB, MKII UK) with $MgK_\alpha$ as an excitation source (the XPS peak positions of each element were corrected by using of C 1s (284.6 eV), UV-Vis diffuse reflectance spectrum with $BaSO_4$ as a substrate, Fluorescence spectra photometer (F-4500) with an excitation wavelength of 340 nm, Transmission electron microscopy (Philips EM400T apparatus) (TEM), and FT-IR using KBr flakes (NEXUS470 spectrophotometer). Identical experiments were also carried out with anatase titania (PW 25, purity $\geq$ 99%) for comparison.

Photocatalytic activity of the samples was investigated by decomposition of methylene blue (hereafter abbreviated as MB) aqueous solution under illumination of electron saving-energy lamp with major emission at 545 nm (Philips, YPZ 220/14-2U.RR.D, 14 W, 760 lm, 23.73 mW/cm$^2$). The initial concentration of MB was 10 mg L$^{-1}$. The dosage of the $TiO_2$ powders was 0.5 g for 500 mL MB solution with the pH value of 7.0. Before switching on irradiation, MB solution was continuously stirred in the dark for 1 h to ensure adsorption–desorption equilibrium. The solution samples were collected from the reactor at regular intervals, centrifuged and analyzed to determine the amounts of residual MB after photo-irradiation, using UV-Vis spectro-photometer (Unico 7200).

The $2 \times 2 \times 1$ $TiO_2$ supercells that possess an anatase crystal structure, $Ti_{16}O_{32}$, $Ti_{16}O_{31}N$, $Ti_{15}FeO_{32}$ and $Ti_{15}FeO_{31}N$, were used for the calculations of electronic structures. The calculations were performed using CASTEP software in Accelrys MS Modelings 3.1 package, in which the GGA and PW91 were introduced for the exchange-correlation function. Meanwhile, ultra-soft pseudo-potential was employed with cut-off energy of 340 eV and reciprocal-space integration over the irreducible Brillouin Zone was approximated at a finite number of k-points using the Monkhorst–Pack scheme with $3 \times 3 \times 2$ k-points grid. The lattice parameters and atomic positions of the supercells were optimized by minimizing the total energy before the calculations of the electronic structures.

## 3. Results and discussion

X-ray diffraction is a method of long-order characterization of solids and heterogeneous catalysts, by which phase composition can be identified and particle size can be estimated using Scherrer equation [19]. XRD patterns of the $TiO_2$-based powders are shown in Fig. 1. The respective average crystallite size obtained with the help of the Scherrer equation is 8–10 nm. It is noticeable that for the N-doped $TiO_2$, the height of the main diffraction peak (1 0 1) is the lowest of these samples, indicating that it possesses smaller crystallite size. As a representative, TEM image of the N-doped $TiO_2$ is given in Fig. 2. The particle size distribution data generated from the TEM micrographs by inspection of 100 particles is shown in Fig. 3. The histogram confirms that most of the particles range from 11 to 16 nm. This is greater than the average crystallite size (8–10 nm) attained from the XRD, which may be caused by their heterocrystal structure. The XRD patterns are found to match that of the anatase phase (JCPDS 21-1272). No peaks corresponding to oxides of iron is observed, such as $Fe_xO_y$, $Fe_xN_y$ and $Fe_xN_yO_z$. Therefore, it can be inferred that either iron ions have been substituted into the crystallite lattice sites of titania or iron oxides exist as a highly dispersed polymeric form over surface, which cannot be detected by XRD [20]. To clarify the state of the doped iron ions, Fourier transform infrared spectra of the PW25 and the as-prepared $TiO_2$ were conducted. It can be seen that in Fig. 4 the FT-IR spectra have identical characteristics, exhibiting a distinct broadband in the 400–900 cm$^{-1}$ region, which have been assigned to bending vibrations of the Ti–O–Ti bond of anatase titania. There is no separate sharp peak at around 1223 cm$^{-1}$ that is a signature peak of the $Fe^{3+}$–$O^{2-}$ stretch in $Fe_2O_3$ [21]. Based on the results, it can be concluded that iron is